Gyrokinetic Theory for Kinetic Analysis of the Resistive Wall Modes in ITER

L.-J. Zheng, M. T. Kotschenreuther, and J. W. Van Dam
Institute for Fusion Studies, University of Texas at Austin, Austin, TX 78712, USA

E-mail contact of main author: lzheng@mail.utexas.edu

Abstract: The current presentation contains two parts: our revisit of the gyrokinetics theory and the application of our newly developed gyrokinetic theory to investigate the resistive wall mode stability in ITER. For the gyrokinetics theory, we explain why part of the conventional gyrokinetics formalism needs to be revamped [1] and show the salient features of our newly derived gyrokinetic equation: 1) recovery of the magnetohydrodynamics (MHD) limit in both perpendicular and parallel directions — not for conventional theory; 2) retrieve of the finite Larmor radius effects missing from the conventional theory. For the application of our theory, we describe our numerical effort to implement our newly developed gyrokinetic equation by extending our existing AEGIS (Adaptive EiGenfunction Independent Solution shooting code) [2] to AEGIS-K codes. The success in recovering full MHD with our newly derived gyrokinetic theory allows us to study the resistive wall modes in a self-consistent nonhybrid kinetic manner. AEGIS-K code is then applied to study the low rotation stabilization of the resistive wall modes in the ITER AT scenario. The particle-wave resonances, the coupling of the shear Alfvén continuum damping, the trapped particle effect, and the parallel electric field effect are all taken into account. Our preliminary numerical results show that the low rotation stabilization of the resistive wall modes in ITER AT scenario with considerable high beta ($f.i.$, $\beta_N = 3$) is achievable.

1. Introduction

Resistive wall mode stability is a major concern for ITER. It has been shown previously that the kinetic and Alfvén resonances can play a significant role in stabilizing the resistive wall modes [3, 4, 5]. However, a fully kinetic analysis of the resistive wall modes is a challenging issue. First, the conventional gyrokinetic equation cannot recover MHD and most existing kinetic MHD codes are hybrid in nature. Second, the coupling of Alfvén continuum damping requires high-resolution computation of the modes at the singular surfaces, which is difficult to achieve with usual non-adaptive codes. Even in the hybrid scheme, it is unclear how the kinetic and Alfvén resonances are coupled and how the parallel electric field affects the stability. All of these issues point to the need for a systematic kinetic analysis of the resistive wall modes in ITER.

Our current effort aims to resolve these difficulties by developing a fully kinetic analysis of the resistive wall modes in ITER. To achieve this goal, the theoretical formalism should, on the one hand, be based on first principles and therefore must be non-hybrid; and on the other hand, should be numerically implementable. Our approach is to derive an extended gyrokinetic formalism that can recover the MHD limit. Our achievement of the recovery of MHD from our newly developed gyrokinetics enables us to extend the MHD stability analyses directly to a fully kinetic analysis without invoking the hybrid kinetic-fluid hypothesis.

Recovering the MHD equations from gyrokinetics is not trivial. We find that the conventional gyrokinetic formalism needs to be significantly modified in order to maintain consistency of ordering and recover the MHD limit. Two major modifications need to be made simultaneously: 1) a sufficiently high-order equilibrium distribution function must be used; 2) the gyrophase-dependent part of the perturbed distribution function and its coupling to the gyrophase-independent part of the perturbed distribution function should be included. The details are outlined in Sec. 2.

The success in recovering full MHD with our newly derived gyrokinetic theory now allows the possibility to study the resistive wall modes in a non-hybrid consistent manner. We implement numerically our newly developed gyrokinetic theory by extending our existing AEGIS [2] to AEGIS-K codes. With the kinetic effect and the coupling of the shear Alfvén resonances taken into account, we are able to study the low rotation stabilization of the resistive wall modes in ITER AT scenario. The numerical work is presented in Sec. 3.

Summary and discussion are given in Sec. 4.

2. Revisit of the linear gyrokinetics theory

The classic electrostatic gyrokinetic formalism was developed in 1960s [6, 7]. Later, the electrostatic gyrokinetics was extended to the electromagnetic one [8, 9]. Most of the gyrokinetic treatments employ the eikonal ansatz for studying the high n modes (n is the toroidal mode number). Recently, a gyrokinetic formalism for long wavelength modes was developed in Ref. [10], in which a great effort has been made to derive the ideal MHD equations from gyrokinetic formalism. The gyrokinetic formalism provides the most efficient way of obtaining the appropriate reduced kinetic equations while still retaining the finite Larmor radius (FLR) effect. However, we show that part of the conventional formalism needs to be revamped in order to recover the ideal MHD and the missing FLR effects. While details have been published in Ref. [1], here we explain only why the conventional linear gyrokinetic theory needs to be corrected, together with the outline of the new features of our newly developed gyrokinetics formalism. There are three reasons to revisit the linear gyrokinetic theory.

First, in the conventional gyrokinetic theory, only the lowest order equilibrium distribution function (*i. e.*, $F_{g0}(\boldsymbol{X}_\perp, \mu, \epsilon)$) is used. Equilibrium distribution function in this order is symmetric with respect to the parallel velocity $v_{||}$ and therefore cannot yield the parallel equilibrium current — the so-called Pfirsch-Schlüter current. This makes the conventional gyrokinetics to be unable to retain the $\boldsymbol{J}_0 \times \delta\boldsymbol{B}$ effect in the perpendicular momentum equation completely. To repair it, the higher order equilibrium distribution function needs to be kept, especially the part of the neoclassical distribution function [11], which gives the Pfirsch-Schlüter current, needs to be kept.

Second, one can easily prove that, even if the neoclassical distribution function is retained, the gyrophase average eliminates this effect. This shows that the gyrophase dependent part of the gyrokinetic distribution function (i.e., the high harmonic components with respect to the gyrophase Fourier decomposition) needs to be solved in order to retain the Pfirsch-Schlüter current effect. There are further reasons to keep the gyrophase-dependent part of the gyrokinetic distribution function. Note that, to compute even (density, pressure) or odd (current) velocity moments in the particle space, one needs to include the gyrophase dependent part of the gyrokinetic distribution function for completeness [12, 13]. We further note that there is coupling between the gyrophase-averaged part and the gyrophase-dependent part of the gyrokinetic distribution function through the term $\dot{\alpha}_1 \partial f/\partial\alpha$, where α is the gyrophase, with subscript "1" denoting the first order and dot representing the derivative along the unperturbed particle orbit. Only this coupling is taken into account, the parallel MHD equation of motion can be retrieved in the proper limit. This coupling also gives rise to additional FLR effects.

Third, we note that the complete gyrophase derivative should be $\dot{\alpha} = -\Omega(\boldsymbol{X}) + \dot{\alpha}_1$, with $\dot{\alpha}_1 = \boldsymbol{v} \cdot \boldsymbol{\nabla}_x \alpha + (1/\Omega)\boldsymbol{v} \times \boldsymbol{e}_b \cdot \boldsymbol{\nabla}_x \Omega$, and $\boldsymbol{\nabla}_x \alpha = (\boldsymbol{\nabla}_x \boldsymbol{e}_2) \cdot \boldsymbol{e}_1 + (v_{||}/v_\perp^2)\boldsymbol{\nabla}_x \boldsymbol{e}_b \cdot (\boldsymbol{v}_\perp \times \boldsymbol{e}_b)$. In the $\dot{\alpha}_1$ expression, the last term is new and results from the guiding center transform of the gyrofrequency $\Omega(\boldsymbol{x})$. This correction is required for ordering consistency. It is due to the inclusion of this correction, the correct MHD parallel equation of motion can be recovered (in $\delta\boldsymbol{A} = \boldsymbol{\xi} \times \boldsymbol{B}$ representation).

The set of our newly derived gyrokinetics and Maxwell equations are given in Ref. [1]. Here, we just outline the new features. First, we have repaired the conventional gyrokinetics formalism, so that the MHD equation can be recovered in the proper limit. Second, we find that the usually used FLR modification of the type $\omega^2 \to \omega(\omega - \omega_{*i})$ in the second order is incomplete. We recover many additional FLR effects. The complexity of the FLR terms is similar in nature to the Braginskii gyroviscous tensor [14]. Actually, the conventional results about FLR effects based on the introduction of the Bessel functions J_0 and J_1 are incomplete in general. We also find that FLR effects in the perturbed collisionless gyrokinetic equation depend on the equilibrium distribution function, which requires collisional closure. We also note that even in the zero-order FLR expansion (*i.e.*, $k_\perp \rho_i \to 0$) our newly derived gyrokinetics equation is different from the conventional drift kinetic equation (see Eq. (2)). This difference results from the inclusion of the coupling of the gyrophase-dependent part of the distribution function through $\dot{\alpha}_1 \partial f / \partial \alpha$ term. We explain the cause for this difference as follows. The definition of the guiding center depends on the choice of the gyrophase. Only the guiding center theory with oscillating part α_1 included in the gyrophase definition can agree with the gyrokinetic theory of the lowest order.

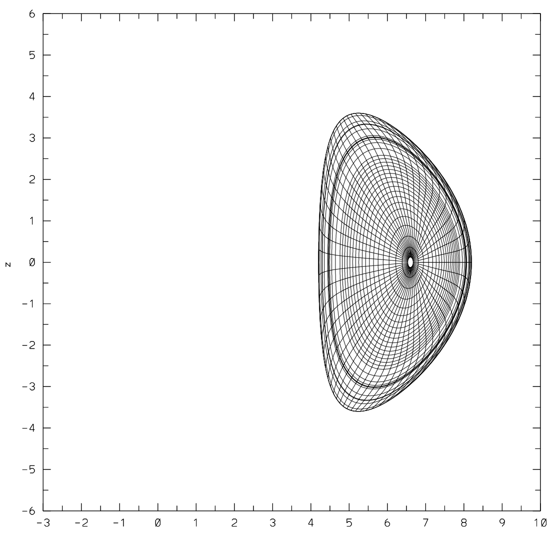

Figure 1: The cross section of the ITER AT configuration with poloidal equal-arc length and radial packed grids shown

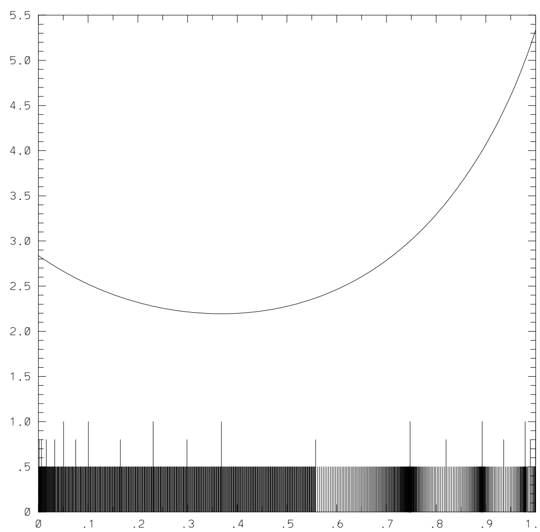

Figure 2: The safety factor profile, with the maximum step size and region separation for shooting shown.

3. Numerical investigation of the resistive wall modes in ITER by AEGIS-K code

In this section we describe our numerical work to implement our newly developed gyrokinetic theory by extending our existing AEGIS [2] to AEGIS-K [15] codes. Since AEGIS formalism is based on the adaptive numerical scheme, we are able to resolve the coupling between the kinetic and the shear Alfvén resonances. For simplicity, we have dropped the FLR effects in our first effort. As discussed in the last section, even in this limit our starting equations are different from the conventional guiding center formalism. The basic set of equations is as follows: the perpendicular momentum equation

$$-\rho_m \omega^2 \boldsymbol{\xi}_\perp = \delta \boldsymbol{J} \times \boldsymbol{B} + \boldsymbol{J} \times \delta \boldsymbol{B} - \boldsymbol{\nabla} \delta P - \boldsymbol{\nabla}_\perp \int d^3 v (m_\rho \mu_0 B) \delta G_0(\boldsymbol{x}), \tag{1}$$

the gyrophase-independent part of the gyrokinetic equation

$$\begin{aligned} & \boldsymbol{v}_{\|} \cdot \boldsymbol{\nabla} G_0(\boldsymbol{X}) - i\omega \delta G_0(\boldsymbol{X}) \\ = \; & i\omega \frac{m_\rho}{T_i} \mu_0 B F_{g0} \boldsymbol{\nabla}_\perp \cdot \boldsymbol{\xi} + i\omega \frac{m_\rho}{T_i} \left(\mu_0 B - v_\|^2\right) F_{g0} \boldsymbol{\kappa} \cdot \boldsymbol{\xi} - i\omega \frac{Ze_i}{T_i} F_{g0} \delta\varphi, \end{aligned} \tag{2}$$

and the quasineutrality condition

$$\delta\varphi \;=\; -\frac{1}{1+Z\tau} \frac{T_e}{Ze_i} \frac{1}{n_0} \int d^3 v \delta G_{0i}. \tag{3}$$

To be specific, we point out that the right hand side of Eq. (2) is different from the conventional guiding center equation. We consider only the low rotation scenario as proposed for ITER. We therefore include the rotation effects by replacing ω with $\omega + n\Omega$ in Eqs. (1) - (3). In our set of equations the wave-particle resonances, the shear Alfvén continuum damping, the trapped particle, and the parallel electric effects are all taken into account. We have not considered the precessional drift resonance as Ref. [5], since we note that considering $\langle\omega_d\rangle$ resonance alone is insufficient for ordering consistency. Noting that $\langle\omega_d\rangle / \omega_{*i} \sim a/R$, inclusion of $\langle\omega_d\rangle$ effect needs also to take into account ω_{*i} effect (i.e., $k_\perp^2 \rho_i^2$ effects) for consistency. Due to this complicity, we postponed this part of work to the next step.

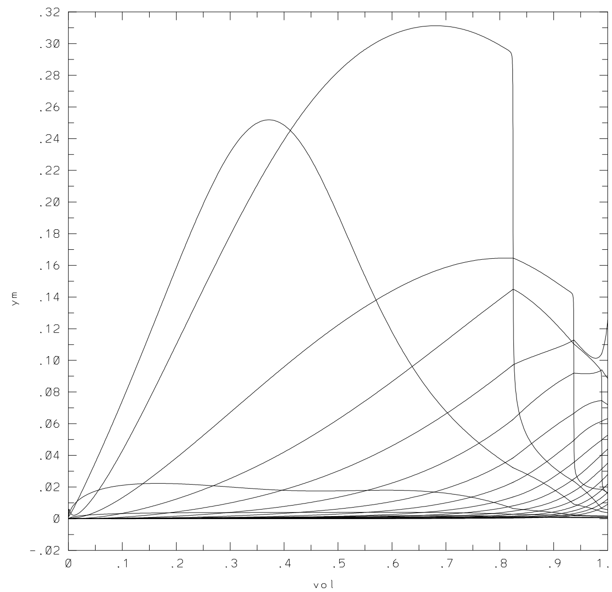

Figure 3: The typical unstable resistive wall modes without rotation computed by AEGIS.

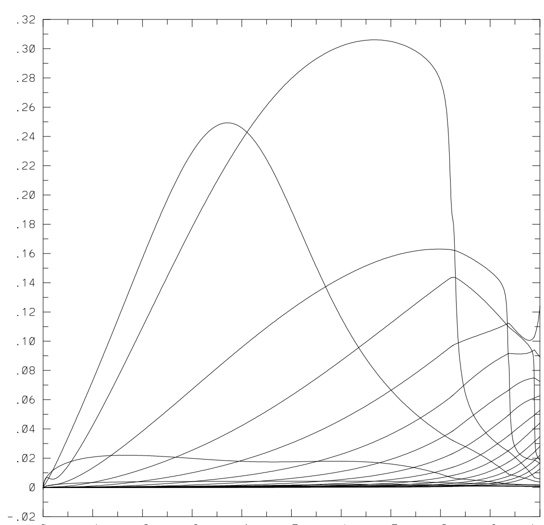

Figure 4: The real part of the unstable resistive wall mode in the presence of rotation.

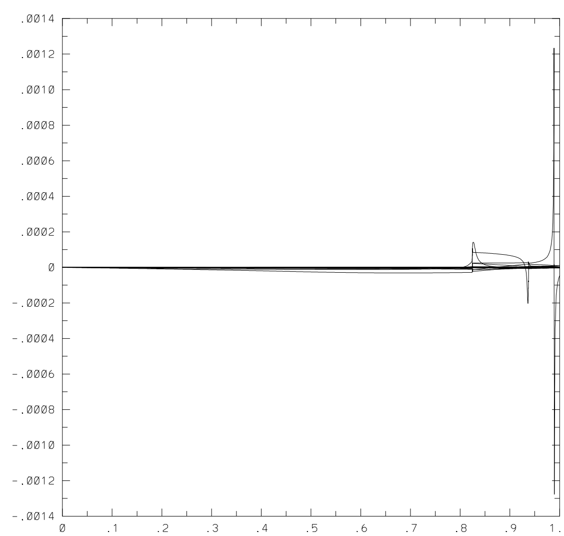

Figure 5: The imaginary part of the unstable resistive wall mode in the presence of rotation.

We consider the ITER AT configuration. The numerical equilibrium is generated by the TOQ code. The case we present here has the following parameters: the average beta $\langle\beta\rangle = 3.41\%$, the beta normal $\beta_N = 3.00\%$, $I/aB = 1.14$, $q_0 = 2.48$, $q_a = 5.34$, $q_{\min} = 2.19$, $q_{95} = 4.19$, the elongation $\kappa_a = 1.8$, and the triangularity $\delta_a = 0.41$. The plasma cross section is given in Fig. 1. The safety factor profile is shown in Fig. 2. At this beta value, the critical ideal wall position is $b = 2.59$. A typical resistive wall mode computed by AEGIS code with parameters: the wall position $b = 1.8$ and the normalized growthrate 1.24 is given in Fig. 3. We note that AEGIS code is in complete agreement with GATO in the ideal MHD computation [1].

With kinetic effects included, we find the rotation stabilization channel. A typical unstable kinetic mode is given in Figs 4 and 5 for the parameters: b=1.8 and normalized growthrate 0.32. One of the advantages of AEGIS-K code lies in that it preserves the ideal MHD roots. This can be seen from the comparison between Fig. 3 and 4. The resistive wall mode growthrates for the $\beta_N = 3.00$ equilibrium described above are plotted in Fig. 6 for various rotation frequencies. Note that in this presentation the rotation frequency is normalized by the Alfvén speed $\sqrt{B^2/(\mu_0\rho R^2 q^2)}$ at the magnetic axis. For normalized rotation frequency about $\Omega = 2 \times 10^{-4}$ a complete stabilization for any wall position can be achieved. In comparing with the results in Ref. [3], the order of this critical rotation frequency seems to be reasonable. This needs to note that the notation frequencies in Ref. [3] is scaled by the apparent mass effect. Using $1 + 2q^2$ as an estimate, this scale is about 20. The product $2 \times 10^{-4} \cdot 20$ is about 0.004. These analyses show also that the effects found in the current kinetic computation is not purely due to the Alfvén continuum damping.

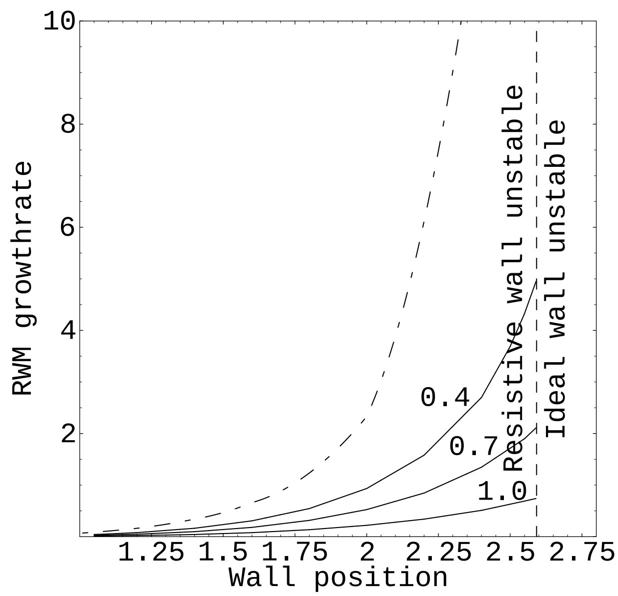

Figure 6: The growth rate versus wall position. The dot dashed curve represents the resistive wall mode growthrate without rotation. The solid curves are the growth rates with the normalized rotation frequency $(\times 10^{-4})$ as parameter.

4. Summary and discussion

In this presentation we outline our newly developed gyrokinetics formalism and describe our application of this new formalism to study the low rotation effect on the resistive wall mode stability in ITER AT scenario with kinetic description.

In the reformulation of the gyrokinetics we point out that three corrections or modifications to the conventional formalism are necessary: (1) the higher order equilibrium distribution function needs to be included; (2) the gyrophase dependent part of the gyrokinetic distribution function needs to be taken into account, and (3) a missing term for the gyrophase expression of the first order needs to be picked up. With these corrections or modifications made, our theory is able to recover the MHD equation both in the perpendicular and parallel directions. Due these corrections or modifications, we also find that the FLR effects are represented by far more terms than the usual results simply by the Bessel functions J_0 and J_1. This helps to explain why the Braginskii gyroviscous tensor is much more complicated than the FLR effects predicted by the conventional gyrokinetic theory.

In the application of our newly derived gyrokinetics theory, we have developed AEGIS-K code. With AEGIS-K, we have studied the low rotation stabilization of the resistive wall modes in the ITER AT scenario with kinetic description. The results are promising. Our preliminary numerical results show that at least for $\beta_N = 3.00$ a full rotation stabilization is possible. AEGIS-K code allows a first ever nonhybrid study of the resistive wall modes in tokamak configuration, with the parallel electric field effect and the coupling of the shear Alfvén resonance taken into account.

Finally, we would like to point out that the significance of our new gyrokinetics theory and AEGIS-K code is beyond the current application to the $n = 1$ resistive wall modes, especially in view of that AEGIS-K is not limited to low-n modes — it is applicable also to the intermediate and high n modes. Besides, the matrix size in the AEGIS numerical scheme is smaller than that based on the usual radial decomposition method. This feature allows AEGIS or AEGIS-K to be extended to 3D application. We also would like to point out that, although AEGIS-K numerical scheme is effective and powerful, the AEGIS-K code is still new. Further tests, especially to compare with the existing codes like MARS, will be carried out in the future.

This research was supported by the Office of Fusion Energy Science of the U.S. Department of Energy under Grant DE-FG02-04ER54742

References

[1] L. J. Zheng, M. T. Kotschenreuther, and J. W. Van Dam, Phys. Plasmas **14**, 072505 (2007).

[2] L. J. Zheng and M. Kotschenreuther, J. Comput. Phys. **221**, 748 (2006).

[3] L. J. Zheng, M. Kotschenreuther, and M. Chu, Phys. Rev. Lett. **95**, 255003 (2005).

[4] A. Bondeson and D. J. Ward, Phys. Rev. Lett. **72**, 2709 (1994).

[5] B. Hu and R. Betti, Phys. Rev. Lett. **93**, 105002 (2004).

[6] P. H. Rutherford and E. A. Frieman, Phys. Fluids **11**, 569 (1968).

[7] J. B. Taylor and R. J. Hastie, Plasma Phys. **10**, 479 (1968).

[8] T. M. Antonsen, Jr. and B. Lane, Phys. Fluids **23**, 1205 (1980).

[9] P. J. Catto, W. M. Tang, and D. E. Baldwin, Plasma Phys. **23**, 639 (1981).

[10] H. Qin and W. M. Tang, Phys. Plasmas **5**, 1052 (2004) and references therein.

[11] R. D. Hazeltine, Advances in Plasma Physics, ed. by A. Simon and W. B. Thompson (John Wiely and Son, Inc., New York, 1976) **6**, 273.

[12] L. Chen and S. T. Tsai, Plasma Phys. **25**, 349 (1983).

[13] S. T. Tsai, J. W. Van Dam, and L. Chen, Plasma Phys. Controlled Fusion **26**, 907 (1984).

[14] S. I. Braginskii, in *Rev. of Plasma Physics*, ed. by M.A. Leontovich (Consultants Bureau, New York, 1965), Vol. **1**, p. 205.

[15] L. J. Zheng, M. T. Kotschenreuther, and J. W. Van Dam, to be submitted to J. Comput. Phys.